Journal of Chromatography B, 879 (2011) 3247–3252

Contents lists available at ScienceDirect

Journal of Chromatography B

journal homepage: www.elsevier.com/locate/chromb

Engineering the substrate specificity of *Alcaligenes* D-aminoacylase useful for the production of D-amino acids by optical resolution☆

Shigekazu Yano[a], Hiroyuki Haruta[a], Takuya Ikeda[a], Takeshi Kikuchi[b], Masahiro Murakami[a], Mitsuaki Moriguchi[c], Mamoru Wakayama[a,*]

[a] Department of Biotechnology, College of Life Sciences, Ritsumeikan University, Kusatsu, 1-1-1 Noji-higashi, Kusatsu, Shiga, 525-8577, Japan
[b] Department of Bioinformatics, College of Life Sciences, Ritsumeikan University, Kusatsu, Shiga, 525-8577, Japan
[c] Department of Food and Bioscience, Beppu University, 82 Kitaishigaki Beppu, Oita 874-8501, Japan

ARTICLE INFO

Article history:
Received 23 November 2010
Accepted 17 March 2011
Available online 14 April 2011

Keywords:
D-Amino acids
Optical resolution
Alcaligenes
D-Aminoacylase
3D model structure

ABSTRACT

D-Aminoacylase from *Alcaligenes xylosoxydans* subsp. *xylosoxydans* A-6 (AxD-NAase) offers a novel biotechnological application, the production of D-amino acid from the racemic mixture of *N*-acyl-DL-amino acids. However, its substrate specificity is biased toward certain *N*-acyl-D-amino acids. To construct mutant AxD-NAases with substrate specificities different from those of wild-type enzyme, the substrate recognition site of the AxD-NAase was rationally manipulated based on computational structural analysis and comparison of its primary structure with other D-aminoacylases with distinct substrate specificities. Mutations of amino acid residues, Phe191, Leu298, Tyr344, and Met346, which interact with the side chain of the substrate, induced marked changes in activities toward each substrate. For example, the catalytic efficiency (k_{cat}/K_m) of mutant F191W toward *N*-acetyl-D-Trp and *N*-acetyl-D-Ala was enhanced by 15.6- and 1.5-folds, respectively, compared with that of the wild-type enzyme, and the catalytic efficiency (k_{cat}/K_m) of mutant L298A toward *N*-acetyl-D-Trp was enhanced by 4.4-folds compared with that of the wild-type enzyme. Other enzymatic properties of both mutants, such as pH and temperature dependence, were the same as those of the wild-type enzyme. The F191W mutant in particular is considered to be useful for the enzymatic production of D-Trp which is an important building block of some therapeutic drugs.

1. Introduction

D-Amino acids have been received much attention because of their usefulness as components of therapeutic drugs, agrochemicals and foods. Regarding the enzymatic methods of synthesizing D-amino acids, the several reports have described the optical resolution of *N*-acyl amino acids by *N*-acyl-D-amino acid amidohydrolase [1], the asymmetric hydrolysis of hydantoins by D-hydantoinase [2], the amination of α-keto acids by a combination of four enzymes (D-amino acid aminotransferase, alanine racemase, alanine dehydrogenase, and formate dehydrogenase) [3], and optical resolution of racemic amino acid amides by D-amino acid amidase [4]. *N*-Acyl-D-amino acid amidohydrolase which catalyzes the hydrolysis of *N*-acyl derivatives of neutral D-amino acids is a so-called D-aminoacylase. The method of D-amino acid production by D-aminoacylase catalysis is expected to be developed further. While L-aminoacylase has been reported in mammals as well as microorganisms, the distribution of D-aminoacylase reported until date is limited to be in some microorganisms such as *Pseudomonas* [5], *Streptomyces* [6], *Alcaligenes* [7–10], *Variovorax* [11], *Defluvibacter* [12], *Trichoderma* [13], and *Microbacterium* [14]. The substrate specificity of D-aminoacylase is dependent on its source, and in general, the enzyme exhibits broad substrate specificity toward *N*-acyl derivatives of neutral D-amino acids. *Alcaligenes xylosoxydans* subsp. *xylosoxydans* A-6 (*Alcaligenes* A-6) produces D-aminoacylase (AxD-NAase). In particular, the enzyme acts preferentially on *N*-acyl derivatives of D-Met, D-Phe, and D-Leu, and less effectively on those of D-Trp, D-Ala, and D-Val. On the other hand, *Alcaligenes* A-6 also produces *N*-acyl-D-aspartate amidohydrolase (AxD-AAase) and *N*-acyl-D-glutamate amidohydrolase (AxD-AGase), which specifically act on *N*-acyl-D-aspartate and *N*-acyl-D-glutamate, respectively [15,16].

For the production of a wide range of D-amino acids by AxD-NAase with a high efficiency, it is necessary to construct a library of mutant enzymes, each of which acts on a certain limited range of substrates with a high catalytic efficiency since it is difficult to create a mutant enzyme which acts on various kinds of substrates with a high catalytic efficiency. The crystal structure of D-aminoacylase

☆ This paper is part of the special issue "Analysis and Biological Relevance of D-Amino Acids and Related Compounds", Kenji Hamase (Guest Editor).

* Corresponding author. Tel.: +81 77 561 2768; fax: +81 77 561 2659.
E-mail address: wakayama@sk.ritsumei.ac.jp (M. Wakayama).

1570-0232/$ – see front matter © 2011 Elsevier B.V. All rights reserved.
doi:10.1016/j.jchromb.2011.03.030

from *Alcaligenes faecalis* DA1 (AfD-NAase) has been recently determined at a high resolution [17,18]. AxD-NAase shows 85% amino acid identity in its primary structure with that of AfD-NAase and also has substrate specificity similar to that of AfD-NAase. We attempted to use a structure-based design as a strategy for understanding the modulation of substrate specificity exerted by the active site residues of AxD-NAase, in order to obtain a library of mutant enzymes that have various substrate specificities and are applicable to the production of a wide range of D-amino acids. A 3D model structure of AxD-NAase was constructed using AfD-NAase as a template for structure modeling. We identified the amino acid residues constituting the hydrophobic pocket accommodating the side chain of the substrate in AxD-NAase. Based on simulation of substrate binding to the enzyme and comparison of the primary structures of the other D-aminoacylases, we constructed the mutant enzymes with substrate specificities different from that of the wild-type enzyme by site-directed mutagenesis. As a result, several mutant enzymes exhibiting different substrate specificity from the wild-type enzyme have been obtained.

In this report, we describe the kinetic properties of F191W and L294A mutant enzymes, which show higher activity toward *N*-acetyl-D-Trp than the wild-type enzyme. The interaction between the substrates and the hydrophobic pockets of these mutant enzymes is also discussed.

2. Experimental

2.1. Materials

N-Acetyl-D-alanine (*N*-Ac-D-Ala), *N*-acetyl-D-valine (*N*-Ac-D-Val), *N*-acetyl-D-leucine (*N*-Ac-D-Leu), *N*-acetyl-D-methionine (*N*-Ac-D-Met), *N*-acetyl-D-tryptophan (*N*-Ac-D-Trp), and *N*-acetyl-D-phenylalanine (*N*-Ac-D-Phe) were purchased from Sigma (MO, USA). The other *N*-acetyl derivatives of D-amino acids and 2,4,6-trinitrobenzenesulfonic acid (TNBS) were from Tokyo Kasei Kogyo Co., Ltd. (Tokyo, Japan). DNA modifying enzymes such as restriction enzymes, DNA ligase, and DNA polymerase were from Takara Bio. The plasmid pKNSD2 was used as an expression plasmid of the wild-type AxD-NAase [16]. QuickChange Site-Directed Mutagenesis Kit was from Stratagene (CA, USA). The other reagents were highest-grade commercial products.

2.2. Construction of model structure

We employed the protein modeling software, Discovery Studio 2.1 (Accelrys, Inc., CA, USA) for the modeling of the 3D structure of AxD-NAase. Structural information on AfD-NAase as a template was obtained from the Protein Data Bank (code 1M7J). The automatic homology modeling program, DS MODELLER was used to prepare the alignment of AxD-NAase and AfD-NAase and to build a 3D model structure of AxD-NAase. After energy minimization, molecular dynamics simulations were performed with the CHARMm potential for 500 ps at 300 K. We set 4.0 for the value of dielectric constant and 8.0 Å cutoff distance for electrostatic and van der Waals energy calculations. The stereochemistry of the model was checked, and all amino acid residues were in allowed conformations. Structures of the wild-type and mutant enzymes with bound substrates were also constructed by MD simulation.

2.3. Site-directed mutagenesis

All mutants were generated using QuikChange Site Directed Mutagenesis Kit according to the instruction of the supplier. The procedure for generation of each mutant utilizes the expression plasmid, pKNSD2 with the gene of wild-type AxD-NAase as a template plasmid and synthetic oligonucleotide primers containing the desired mutation listed in Table 1. The oligonucleotide primers, each complementary to opposite strands of the plasmid, were extended by *Pfu* Turbo DNA polymerase. All mutants were sequenced to confirm the mutation introduced using an automatic DNA sequence analyzer, the DSQ-2000L system (Shimadzu Biotech, Kyoto, Japan).

2.4. Expression and purification of the enzymes

Escherichia coli JM109 was used as a host strain of recombinant plasmids for the wild-type and mutant enzymes. Each transformant was grown in 2-l Luria–Bertani broth containing 50 μg/ml of ampicillin with 0.1 mM of isopropyl β-D-thiogalactopyranoside at 30 °C for 20 h with shaking at 200 r.p.m. Cells harvested in 10 mM potassium phosphate buffer (pH 7.0) was disrupted by sonication and the supernatant obtained by centrifugation was dialyzed against the buffer. Then, the cell-free extract prepared was used for enzyme purification. All column chromatography steps were done at 0–8 °C and 10 mM potassium phosphate buffer (pH 7.0) was used unless otherwise stated. The cell-free extract was applied to a DEAE-Toyopearl column (4 cm × 28 cm) equilibrated with the buffer. After washing the column with the buffer containing 50 mM NaCl, the enzyme was eluted with the buffer containing 100 mM NaCl. The active fractions were collected and concentrated by ultrafiltration with Amicon PM-10 membrane. After glycerol (10%), 2-mercaptoethanol (0.01%), and 0.01 mM $ZnCl_2$ were added to the enzyme solution, solid ammonium sulfate was added to the enzyme solution to give 20% saturation. The enzyme solution was applied to a Butyl-Cellulofine column (2 cm × 8 cm) previously equilibrated with the buffer containing 20% ammonium sulfate, 10% glycerol, 0.01% 2-mercaptoethanol, and 0.01 mM $ZnCl_2$. The column was washed with the buffer containing 15% ammonium sulfate and the enzyme was eluted with the buffer containing 10% ammonium sulfate. The enzyme collected was dialyzed against the buffer and then concentrated by ultrafiltration [19]. The wild-type and mutant enzymes were purified in a homogeneous state as judged by SDS-PAGE. CD spectra of the purified wild-type and mutant enzymes (0.1 mg/ml) were measured at 25 °C with a 1-cm light path cell in the far-UV region (200–280 nm) under a nitrogen atmosphere with a Jasco spectropolarimeter model J-720. The other conditions of CD spectra were as follows, data interval; 0.5 nm, scan speed; 100 nm/min, accumulation times; 3, band width; 2.0 nm, and sensitivity; 100 mdeg.

2.5. Assay and kinetic measurements

Enzyme activity was determined by using a standard reaction mixture containing 100 mM HEPES buffer (pH 7.0), 20 mM *N*-acetyl-D-amino acids, and the enzyme in the final volume of 0.2 ml. After incubating at 30 °C for 10 min, the reaction was terminated by adding 0.10 ml of 0.25 M NaOH solution to the reaction mixture. The liberated D-amino acid was determined by its reaction with 2,4,6-trinitrobenzenesulfonic acid (TNBS) [20]. Continuously, 100 μl of 125 mM NaB_4O_7 solution and 40 μl if 200 mM TNBS solution were added to the reaction mixture in this order, and then incubated at 30 °C for 10 min. Finally, 800 μl of $NaH_2PO_4{\cdot}Na_2SO_3$ solution was added to the reaction mixture. The absorbance at 520 nm was measured. One unit of enzyme activity was defined as the amount of enzyme which catalyzed the formation of 1 μmol of D-amino acid per min. Protein was estimated by the method of Lowry et al. with crystalline egg albumin as a standard. Kinetic constants for various substrates of the wild-type and mutant enzymes were determined with a double-reciprocal plot of the measured initial reaction rates and substrate concentration (8–300 mM).

Table 1
Primers used in site-directed mutagenesis.

Mutation	Direction	Mutagenic oligonucleotide
F191W	Forward	5′-ggcatttcgaccggcgcctggtacccgcccgcc-3′
	Reverse	5′-ggcgggcgggtaccaggcgccggtcgaaatgcc-3′
V297F	Forward	5′-ctcaagcaggaccgcttcgcactggccggacgcaccatc-3′
	Reverse	5′-gatggtgcgtccggccagtgccacgcggtcctgcttgag-3′
L298F	Forward	5′-gcgtccggccagaaacacgcggtcctg-3′
	Reverse	5′-caggaccgcgtgtttctggccggacgc-3′
L298A	Forward	5′-ctcaagcaggaccgcgtggcactggccggacgcaccatc-3′
	Reverse	5′-gatggtgcgtccggccagtgcgaagcggtcctgcttgag-3′
M346F	Forward	5′-gccatctacttcttcatggacgaaccgac-3′
	Reverse	5′-gtcgggttcgtccatgaagaagtagatggc-3′

The codons corresponding to the substituted amino acids are underlined.

3. Results and discussion

3.1. Analysis of substrate-binding pocket of AxD-NAase

The 3D structure of AxD-NAase was constructed by homology modeling with AfD-NAase as a template. The amino acid residues of AxD-NAase, that differ from those of AfD-NAase in the amino acid sequence, were evaluated by Ramachandran plot, and consequently no amino acid residue was found unsuitable. The enzyme consists of β-sheets at both the *N*- and the *C*-terminals and a α/β barrel in the center of the enzyme including the active site. A 63-amino acid residues insertion (residues 285–347), which is thought to be a gate controlling access to the active site of AfD-NAase, was also conserved in AxD-NAase like AfD-NAase. The overall structure of AxD-NAase was clarified to be homologous to that of AfD-NAase in fine detail (data not shown).

Because the structure of the active site of AxD-NAase was well matched with that of AfD-NAase, structural coordination of the substrate and active site of the enzyme was achieved in the same way as that for AfD-NAase [17]. *N*-Acetyl-D-Met, one of the preferred substrates, was used as a substrate. It has been reported that there are specific sites for the binding of two acetate molecules in the active center of AfD-NAase. One site existing near the essential zinc ion is the binding site of acetate produced in the hydrolysis of *N*-acetyl-D-amino acid, and the other is the binding position of the carboxylate group of the substrate. According to the binding-way of acetate described in the paper [17], the preferred substrate *N*-acetyl-D-Met was modeled into the active site of AxD-NAase. Then, the side chain was docked at the hydrophobic pocket. The α-carboxyl and *N*-acetyl amide groups were fixed and a conformation optimized by the energy minimization was used as the starting conformation for molecular dynamics (MD) simulation using DS CHARMm. The predicted active site structure of wild-type AxD-NAase with *N*-Ac-D-Met is shown in Fig. 1. In this case, the steric arrangement of the substrate, Asp366 (essential for catalysis), and the zinc ion in the active site is considered to be ideal to provide a high hydrolytic activity toward the *N*-acetyl amide bond of the substrate. This structure modeling revealed that the amino acid residues constituting the hydrophobic substrate-binding pocket were determined to be Phe191, Tyr192, Met221, Glu224, Lys252, Met254, Thr290, Val297, Leu298, Tyr344, and Met346 (Fig. 2).

3.2. Mutant design

To determine the target amino acid residues for substitution, the primary structure of AxD-NAase was compared with that of D-aminoacylase from *Variovorax paradoxus* (VpD-NAase), which shows relatively high activity toward *N*-acetyl-D-Ala and *N*-acetyl-D-Val. This revealed that Phe191, Val297, Leu298, and Met346 among the amino acid residues constituting the substrate-binding pocket of AxD-NAase were substituted with the amino acid residues, Trp, Asp, Met, and Phe, respectively in VpD-NAase. Side chains of these amino acid residues of AxD-NAase are oriented to the inside of the pocket and interact with *N*-acetyl-D-Met (Fig. 2). On the other hand, replacement of these amino acid residues by bulky amino acid residues in VpD-NAase might make the pocket smaller such that *N*-acetyl-D-Ala and *N*-acetyl-D-Val with the small side chains become good substrates. Then, we substituted the amino acid residues, F191, V297, L298, and M346 with W191,

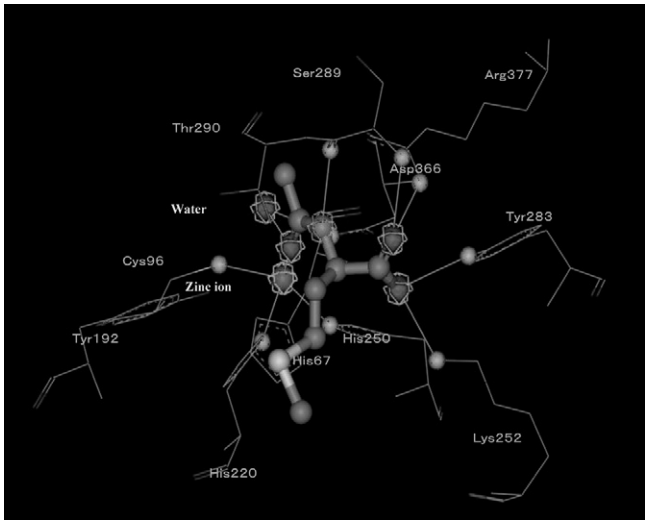

Fig. 1. The predicted catalytic site structure of wild-type D-aminoacylase from *Alcaligenes* A-6 with *N*-acetyl-D-methionine.

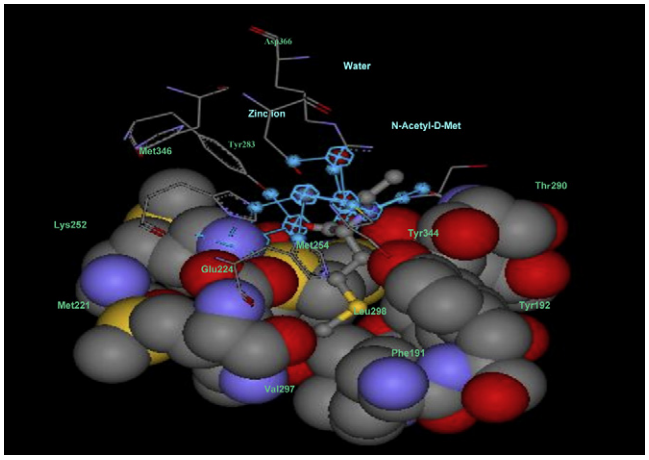

Fig. 2. The space filling model of the predicted catalytic site of D-aminoacylase from *Alcaligenes* A-6 with *N*-Ac-D-Met. Side chain of the substrate, *N*-acetyl-D-methionine interacts with the amino acid residues forming hydrophobic pocket in the active site.

F297, F298, and F346, respectively in AxD-NAase in order to obtain mutant enzymes exhibiting high substrate preference for *N*-acetyl-D-Ala and *N*-acetyl-D-Val. Furthermore, we also substituted L298 with A298 in AxD-NAase to obtain a mutant enzyme exhibiting high preference to the substrate with the bulky side chains such as *N*-acetyl-D-Trp. Especially, both V297 and L298 were substituted with phenylalanine having more bulky side chain than those of aspartic acid and methionine residues. Since both V297 and L298 occupy the space around the bottom of hydrophobic pocket, the replacement of these amino acid residues by the amino acids with more bulky or smaller side chains was expected to give significant changes of substrate preference to mutant enzymes.

3.3. Expression and purification of the mutant enzymes

All mutant enzymes were well expressed in the cell-free extract with the same expression level as the wild-type enzyme, and the wild-type enzyme as well as mutant enzymes were purified to homogeneity as per SDS–PAGE analysis; the molecular mass of each subunit was 52 kDa and was the same for the wild-type and mutant enzymes (data not shown). All mutant enzymes gave circular dichroism (CD) spectra similar to that of the wild-type enzyme, suggesting that the replacement of Phe191, V297, Leu298, and Met346 with Trp, Phe, Ala, or Phe did not significantly influence the content of the secondary structure of the mutant enzymes (Fig. 3).

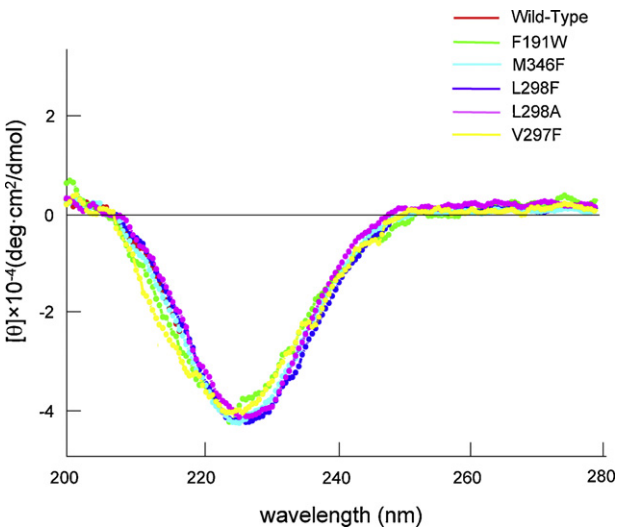

Fig. 3. CD spectra of wild-type and mutant AxD-NAases (For interpretation of the references to color in this figure legend, the reader is referred to the web version of the article.).

3.4. Kinetic properties of F191W and L298A mutant enzymes

To investigate the influence of amino acid residues on the substrate specificity, Phe191, Val297, Leu298, and Met346 located in the substrate-binding pocket of AxD-NAase were mutated to smaller or larger amino acids by referring D-aminoacylase of *V. paradoxus*. Activities of mutant enzymes with respect to given substrates were determined (Fig. 4). Both M346F and L298F showed rather lower activities toward all substrates tested including *N*-acetyl-D-Met compared with the wild-type enzyme. V297F showed partially lower activities toward all substrates tested compared with the wild-type enzyme. On the other hand, both F191W and L298A exhibited higher catalytic activity toward *N*-acetyl-D-Trp than the wild-type enzyme. The activity of F191W on *N*-acetyl-D-Ala was also improved. Table 2 shows the kinetic parameters of these two mutants for *N*-acetyl-D-Met, *N*-acetyl-D-Trp, and *N*-acetyl-D-Ala. The catalytic efficiency of L298A for *N*-acetyl-D-Met and *N*-acetyl-D-Ala decreased to between 1/40 and 1/20 of that of the wild-type enzyme, respectively. This was caused by decreases in both K_m and k_{cat} toward *N*-acetyl-D-Met and *N*-acetyl-D-Ala. However, the catalytic efficiency of L298A toward *N*-acetyl-D-Trp increased about 4.3 fold, indicating that the change was caused by increases in both K_m and k_{cat} toward the substrate. F191W retained its catalytic efficiency toward *N*-acetyl-D-Met compared with that of the wild-type enzyme. In addition, efficiency toward *N*-acetyl-D-Trp and *N*-acetyl-D-Ala increased about 15.6- and 1.5-fold, respectively. This improvement in catalytic efficiency toward both substrates was caused by the increases in K_m and k_{cat}.

In the present study, we substituted the amino acid residues F191 and L298, which are located at the bottom of the substrate-binding pocket, with Trp and Ala, respectively. In the resultant mutant enzymes, F191W and L298A, the catalytic efficiency toward *N*-acetyl-D-Trp was highly improved. However, no improvement of the catalytic efficiency toward *N*-acetyl-D-Ala in F191W was observed although Phe at the position 191 was substituted with Trp after the model of D-aminoacylase from *V. paradoxus* with relatively high catalytic efficiency toward *N*-acetyl-D-Ala. These results indicate that bulkiness of the amino acid at position of both 191 and 298 of AxD-NAase is important in the recognition of substrate. Recently, Cummings et al. reported that Gox1177 from *Gluconobacter oxidans* and Sco4986 from *Streptomyces coelicolor* exhibited D-aminoacylase activity [21]. Both Gox1177 and Sco4986 have

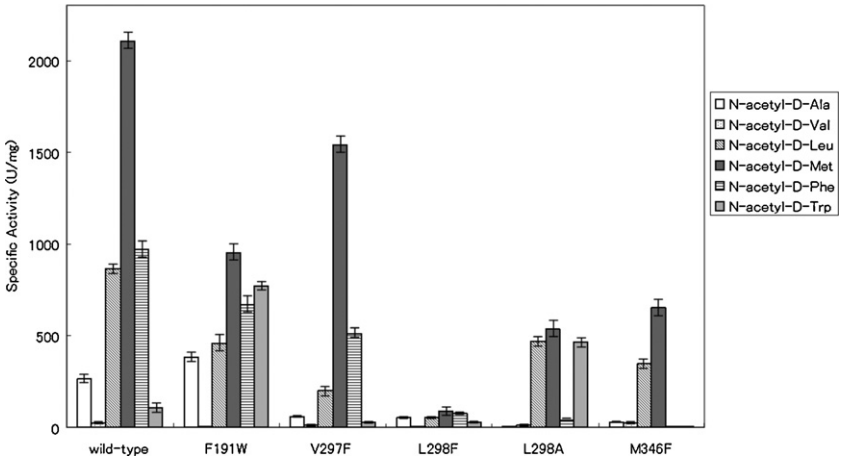

Fig. 4. Comparison of specific activities of wild-type and mutant AxD-NAases toward various substrates, *N*-Ac-D-Ala, *N*-Ac-D-Val, *N*-Ac-D-Leu, *N*-Ac-D-Met, *N*-Ac-D-Phe, and *N*-Ac-D-Trp. The data are expressed as mean ± SE ($n = 3$).

Table 2
Kinetic constants of wild-type and mutant AxD-NAases.

Enzyme	N-Ac-D-Met			N-Ac-D-Trp			N-Ac-D-Ala		
	K_m (mM)	k_{cat} (s^{-1})	k_{cat}/K_m (s^{-1}/mM)	K_m (mM)	k_{cat} (s^{-1})	k_{cat}/K_m (s^{-1}/mM)	K_m (mM)	k_{cat} (s^{-1})	k_{cat}/K_m (s^{-1}/mM)
Wild-type	4.80	1826	381	6.23	89.5	14.4	41.0	229	5.58
F191W	2.03	829	407	2.97	669	225	38.6	330	8.56
L298A	56.4	463	8.21	6.36	404	63.5	330	5.97	0.02

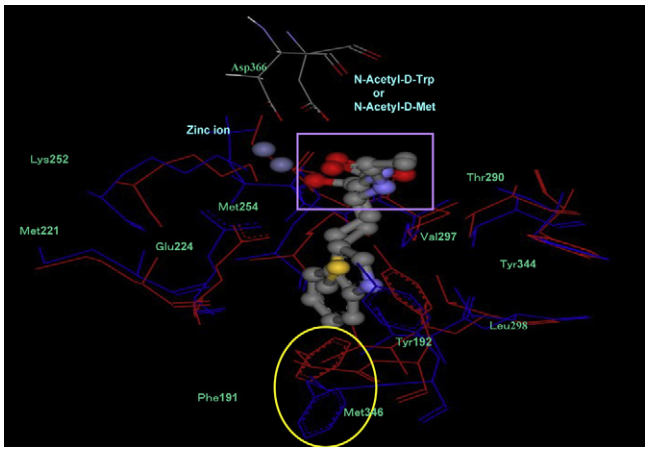

Fig. 5. Superposition of the substrate binding pockets in the wild-type AxD-NAase with the preferred substrate, *N*-Ac-D-Met and with the poor substrate, *N*-Ac-D-Trp, shown in red and blue, respectively. The immobilized portion of the substrate expediently and the shift of Phe191 residue by entrance of the side chain of *N*-Ac-D-Trp into the substrate-binding pocket were indicated by a rectangle and an oval, respectively. (For interpretation of the references to color in this figure legend, the reader is referred to the web version of the article.)

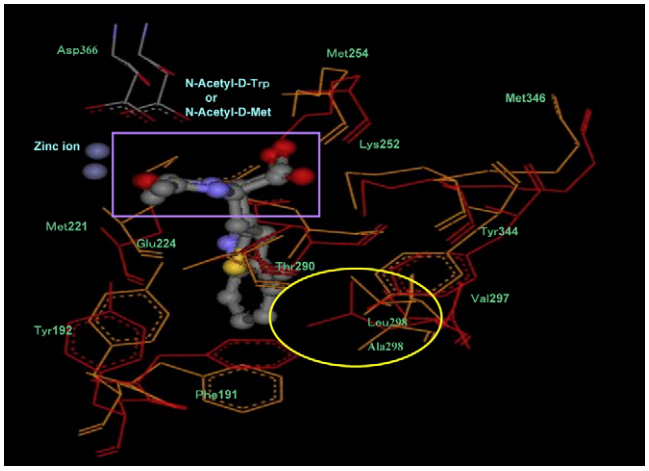

Fig. 6. Superposition of the substrate binding pockets in the wild-type AxD-NAase with *N*-Ac-D-Met and in the L298A mutant enzyme with *N*-Ac-D-Trp, shown in red and orange, respectively. The immobilized portion of the substrate expediently and the position of substituted amino acid residue were indicated by a rectangle and an oval, respectively. (For interpretation of the references to color in this figure legend, the reader is referred to the web version of the article.)

substrate specificity different from those of D-aminoacylases from *Alcaligenes* sp. and *N*-acetyl-D-Trp is one of preferred substrates for both Gox1177 and Sco4986. In particular, the catalytic efficiency of Gox1177 toward *N*-acetyl-D-Trp ($k_{cat}/K_m = 4.1 \times 10\ mM^{-1}\ s^{-1}$) is 2.8-fold higher than that of the wild-type AxD-NAase but is 1/5.5 of that of the F191W mutant.

3.5. Interaction between the substrates and the hydrophobic pocket of mutant enzymes

Fig. 5 shows the model structures of the wild-type enzyme–substrate complex with the preferred substrate, *N*-acetyl-D-Met and a poor substrate, *N*-acetyl-D-Trp. In this model, the side chains of both substrates were introduced in the hydrophobic pocket of the active site of the enzyme in such a way that the *N*-acetyl and carboxylic groups of the α-carbon atom of the substrate were fixed in an ideal orientation for a catalytic reaction. In this case, as shown in Fig. 5, when the substrate N-Ac-D-Met binds to the active site of the wild-type enzyme, the steric positions of the amino acid residues such as Phe191 and Tyr192 shift outside, so that the cleft at the active site is widened. When the substrate enters the active site of AxD-NAase, the structure of the active site is considered to change. The side chain of the F191 residue in the wild-type enzyme–*N*-acetyl-D-Trp complex oriented much more to the outer side of the pocket compared with that in wild-type–*N*-acetyl-D-Met complex. This indicates that large steric hindrance between the F191 residue and the side chain of *N*-acetyl-D-Trp occurs when *N*-acetyl-D-Trp is introduced into the active site. In fact, because the *N*-acetyl and α-carboxyl groups of the substrate are not fixed, the susceptible amide bond of *N*-acetyl-D-Trp is pushed away from the proper position for catalysis as a result of steric hindrance. Consequently, the relationship between the positions of the *N*-acetyl group, Asp366 residue, and zinc ions involved in catalysis in the case of *N*-acetyl-D-Trp might be different from that in the case of *N*-acetyl-D-Met. This is the reason why the wild-type enzyme exhibits lower activity toward *N*-acetyl-D-Trp than toward *N*-acetyl-D-Met. The L298A mutant–*N*-acetyl-D-Trp complex was superimposed on the wild-type enzyme–*N*-acetyl-D-Met complex (Fig. 6). L298 is one of the amino acid residues located at the bottom of the active

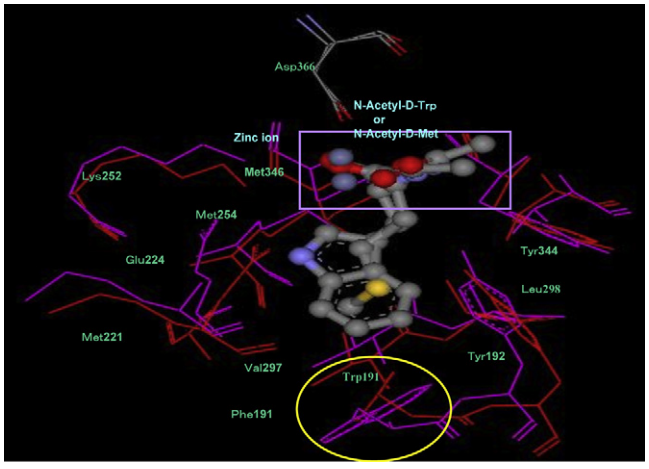

Fig. 7. Superposition of the substrate binding pocket in the wild-type AxD-NAase with *N*-Ac-D-Met and in the F191W mutant enzyme with *N*-Ac-D-Trp, shown in red and purple, respectively. The immobilized portion of the substrate expediently and the position of substituted amino acid residue were indicated by a rectangle and an oval, respectively. (For interpretation of the references to color in this figure legend, the reader is referred to the web version of the article.)

site pocket and beside F191. The substitution of Ala with Leu at the position of 298 provides the space to take in the side chain of *N*-acetyl-D-Trp. Consequently, steric hindrance between the F191 residue and the side chain of *N*-acetyl-D-Trp is reduced and the positional relationship of the *N*-acetyl group, Asp366 residue, and zinc ions involved in catalysis in the case of *N*-acetyl-D-Trp might be similar to that in the case of *N*-acetyl-D-Met, resulting in improvement of catalytic efficiency toward *N*-acetyl-D-Trp. Similarly, the F191W mutant–*N*-acetyl-D-Trp complex was superimposed on the wild-type enzyme–*N*-acetyl-D-Met complex (Fig. 7). In the wild-type enzyme, the decrease in catalytic activity might be caused by the steric hindrance between Phe191 and the side chain of *N*-acetyl-D-Trp, the substrate. However, in the F191W mutant, the substitution of Trp with Phe at position 191 produces a side space in the pocket by pushing Met221 and Glu224 out, and then the side chain of *N*-acetyl-D-Trp can enter the space produced. Consequently, the susceptible amide bond of *N*-acetyl-D-Trp could be positioned properly for catalysis in the relation to the Asp366 residue and zinc ions, leading to increased catalytic efficiency toward *N*-acetyl-D-Trp.

Several enzymes have been used for industrial applications in various fields, but it is often the case that their substrate specificities are unfavorable for practical purposes. D-Amino acid production using D-aminoacylase is such a case. In this study, we modeled the 3D structure of D-aminoacylase from *Alcaligenes* A-6 and estimated the changes of catalytic properties of mutant enzymes with MD simulation. Similar approaches on the structure and function of enzymes with MD simulation analysis have been reported [22,23]. Consequently, we obtained mutant enzymes with desirable properties, and discussed the relationship between the substrate specificity and conformation of the substrate-binding pocket in D-aminoacylase. D-Trp is an amino acid that is in high demand industrially, and the mutant enzymes obtained in this study may contribute to the effective production of D-Trp.

References

[1] Y.C. Tsai, C.S. Lin, T.H. Tseng, H. Lee, Y.J. Wang, Enzyme Microb. Technol. 14 (1992) 384.
[2] Y.H. Cheon, S. Kim, K.H. Han, J. Abendroth, K. Niefind, D. Schonburg, J. Wang, Y. Kim, Biochemistry 41 (2002) 9410.
[3] A. Galkin, L. Kulakova, T. Yoshimura, K. Soda, N. Esaki, Appl. Environ. Microbiol. 63 (1997) 4651.
[4] T. Hongpattaakere, H. Komeda, Y. Asano, J. Ind. Microbiol. Biotechnol. 32 (2005) 567.
[5] Y. Kameda, T. Hase, S. Kanatomo, Chem. Pharm. Bull. 26 (1978) 2698.
[6] M. Sugie, H. Suzuki, Agric. Biol. Chem. 44 (1980) 1089.
[7] M. Moriguchi, K. Sakai, Y. Miyamoto, M. Wakayama, Biosci. Biotechnol. Biochem. 57 (1993) 1149.
[8] M. Moriguchi, K. Ideta, Appl. Environ. Microbiol. 54 (1988) 2767.
[9] Y.C. Tsai, C.P. Tseng, K.M. Hsiao, L.Y. Chen, Appl. Environ. Microbiol. 54 (1988) 984.
[10] Y.B. Yang, C.S. Lin, C.P. Tseng, Y.J. Wang, Y.C. Tsai, Appl. Environ. Microbiol. 57 (1991) 1259.
[11] P.H. Lin, S.C. Su, Y.C. Tsai, C.Y. Lee, Eur. J. Biochem. 269 (2002) 4868.
[12] S. Kumagai, M. Kobayashi, S. Yamaguchi, T. Kanaya, R. Motohashi, K. Isobe, J. Mol. Catal. B: Enzym. 30 (2004) 159.
[13] M. Wakayama, S. Kitahata, L. Manoch, T. Tachiki, K. Yoshimune, M. Moriguchi, Process Biochem. 39 (2004) 1119.
[14] J. Liu, T. Nakayama, H. Hemmi, Y. Asano, N. Tsuruoka, K. Shimomura, M. Nishijima, T. Nishino, Int. J. Syst. Evol. Microbiol. 55 (2005) 661.
[15] M. Moriguchi, K. Sakai, Y. Katsuno, T. Maki, M. Wakayama, Biosci. Biotechnol. Biochem. 57 (1993) 1145.
[16] K. Sakai, K. Imamura, Y. Sonoda, H. Kido, M. Moriguchi, FEBS Lett. 289 (1991) 44.
[17] S.H. Liaw, S.J. Chen, T.P. Ko, C.S. Hsu, C.J. Chen, A.H.J. Wang, Y.C. Tsai, J. Biol. Chem. 278 (2003) 4957.
[18] W.L. Lai, L.Y. Chou, C.Y. Ting, R. Kirby, Y.C. Tsai, A.H.J. Wang, S.H. Liaw, J. Biol. Chem. 279 (2004) 13962.
[19] M. Wakayama, S. Hayashi, Y. Yatsuda, Y. Katsuno, K. Sakai, M. Moriguchi, Protein Express. Purif. 7 (1996) 395.
[20] R. Konno, H. Bruckner, A. D'Aniello, G. Fisher, N. Fuji, H. Homma (Eds.), d-Amino Acids, Nova Biomedical Books, New York, 2008, p. 564.
[21] J.A. Cummings, A.A. Fedorov, C. Xu, S. Brown, E. Fedorov, P.C. Babitt, S.C. Almo, F.M. Raushel, Biochemistry 48 (2009) 6469.
[22] C.S. Hsu, W.L. Lai, W.W. Chang, S.H. Liaw, Y.C. Tsai, Protein Sci. 11 (2002) 2545.
[23] K. Suzukawa, T. Yamagami, T. Ohmura, H. Hirakawa, S. Kuhara, Y. Aso, M. Ishiguro, Biosci. Biotechnol. Biochem. 67 (2003) 341.